

1 HDC1 interacts with SHL1 and H1

2
3 Corresponding author: Anna Amtmann, Plant Science Group, MCSB, MVLS, University of
4 Glasgow, Glasgow G12 8QQ, UK

5
6 **The Histone Deacetylase Complex (HDC) 1 protein of *Arabidopsis thaliana* has the capacity to**
7 **interact with multiple proteins including histone 3-binding proteins and histone 1 variants.**

8
9 Giorgio Perrella¹, Craig Carr¹, Maria A. Asensi-Fabado¹, Naomi A. Donald¹, Katalin Páldi^{1,3},
10 Matthew A. Hannah², Anna Amtmann^{1*}

11
12 ¹Plant Science Group, MCSB, MVLS, University of Glasgow, Glasgow G128QQ, UK

13 ²Bayer CropScience NV, Technologiepark 38, B-9052 Gent, Belgium

14
15 **1-sentence summary:**

16 A conserved ancestral domain of the intrinsically disordered protein HDC1 can directly interact
17 with H3-binding proteins and with H1 variants, thus providing a means for mediating between
18 histones at the core-nucleosome and at the linker DNA.

19
20 **Author contributions:**

21 G. P. performed and analysed most of the experiments. C. C. and K. P. assisted with the BiFC
22 assays, M.A.A. quantified leaf phenotypes and N. A. M. assisted with cloning and transformation.
23 G.P., M.A.H. and A.A. planned the experiments. A.A. wrote the paper with input from all authors.

24
25 **Funding:**

26 This work was supported by an Industrial Partnership Award from the Biotechnology and
27 Biological Sciences Research Council (BBSRC grant no. BB/K008218/1 to A.A.). M.A.A. was
28 funded by a Marie Curie fellowship from the European Commission (IEF No. 627658 to M.A.A.)

29
30 ³Present address: GMI, Bohrgasse 3, 10130 Vienna, Austria

31
32 *Correspondence should be addressed to Anna Amtmann (anna.amtmann@glasgow.ac.uk)

36 **ABSTRACT**

37 Intrinsically disordered proteins can adopt multiple conformations thereby enabling interaction with
38 a wide variety of partners. They often serve as hubs in protein interaction networks. We have
39 previously shown that the Histone Deacetylase Complex (HDC) 1 protein from *Arabidopsis*
40 *thaliana* interacts with histone deacetylases and quantitatively determines histone acetylation levels,
41 transcriptional activity and several phenotypes, including ABA-sensitivity during germination,
42 vegetative growth rate and flowering time. HDC1-type proteins are ubiquitous in plants but they
43 contain no known structural or functional domains. Here we explored the protein interaction
44 spectrum of HDC1 using a quantitative BiFC assay in tobacco epidermal cells. In addition to
45 binding histone deacetylases, HDC1 directly interacted with histone H3-binding proteins and co-
46 repressor associated proteins, but not with H3 or the co-repressors themselves. Surprisingly, HDC1
47 was also able to interact with variants of the linker histone H1. Truncation of HDC1 to the ancestral
48 core sequence narrowed the spectrum of interactions and of phenotypic outputs but maintained
49 binding to a H3-binding protein and to H1. Thus HDC1 provides a potential link between H1 and
50 histone modifying complexes.

51

52

53 INTRODUCTION

54 Regulation of gene transcription underpins plant development and dynamic responses to the
55 environment. Transcription occurs in the context of chromatin, a highly condensed structure in
56 which the DNA is wrapped around nucleosomes comprised of histone octamers comprised of
57 histones H2A/B, H3 and H4, and further stabilised by linker histone H1 (Over and Michaels, 2014;
58 Hergeth and Schneider, 2015). Alteration of chromatin structure plays an important part in
59 transcriptional regulation and is achieved through multi-protein complexes that recognize and
60 instigate biochemical modifications of the DNA and/or the histones (Pfluger and Wagner, 2007;
61 Derkacheva et al., 2013). For example, binding of repressors to so-called co-repressors recruits
62 histone deacetylases (HDAs) to the gene region (Song et al., 2005). The HDAs in turn interact with
63 histone binding proteins (Mehdi et al., 2015). Removal of acetyl groups from lysine residues of the
64 core histones leads to chromatin compaction and inhibition of transcription (Kouzarides, 2007;
65 Roudier et al., 2009). Specific recruitment at both ‘ends’ of the repressive protein complex
66 generates a double lock between DNA and the nucleosome: the repressors recognize certain DNA-
67 motifs in the gene promoters and the histone-binding proteins recognize (‘read’) certain histone
68 residues and their modifications (Liu et al., 2010). A minimal HDAC complex therefore needs to
69 combine at least three protein functions; repressor-binding, histone-binding and catalytic activity.
70 Biochemical studies in yeast and in animal systems have provided evidence for large multi-protein
71 complexes linking a co-repressor and a histone deacetylase with several histone-binding proteins
72 and a range of associated proteins of mostly unknown functions (Yang and Seto, 2008). Plant
73 HDAC complexes are less well characterised but in a recent study several proteins, including co-
74 repressors and histone-binding proteins, were found to co-precipitate with a histone deacetylase,
75 suggesting that the basic composition of plant HDAC complexes is similar to that of animal and
76 yeast complexes (Mehdi et al., 2015).

77 Histone Deacetylation Complex 1 (HDC1) protein is an important component of the plant
78 HDAC machinery (Perrella et al., 2013). We have reported that knockout of HDC1 in *A. thaliana*
79 promotes histone acetylation and gene expression, and causes a range of phenotypes, most notably
80 hypersensitivity to abscisic acid (ABA) during germination, inhibition of leaf growth and delayed
81 flowering (Perrella et al., 2013). Conversely, over-expression of HDC1 desensitized the plants to
82 ABA and increased shoot biomass even in water-limited conditions. Thus, HDC1 appeared to be a
83 rate-limiting factor of HDAC. HDC1 is a component of native HDAC complexes in *A. thaliana*
84 (Derkacheva et al., 2013; Mehdi et al., 2015) and it directly interacts with the histone deacetylases
85 HDA6 and HDA19 (Perrella et al., 2013). Both HDAs have previously been reported to function in
86 germination (Tanaka et al., 2008; Yu et al., 2011), flowering (Tanaka et al., 2008; Yu et al., 2011)
87 and ABA-mediated responses to drought or salt (Chen et al., 2010; Chen and Wu, 2010). The

88 phenotypes of HDC1 mutants can therefore be explained by HDC1 acting through these HDAs, but
89 the mechanism by which HDC1 controls their apparent activity remains to be elucidated.

90 HDC1 is a ubiquitously expressed single-copy gene in Arabidopsis, and HDC1 homologs
91 are present across the plant kingdom as single or low-copy genes. The HDC1 sequence contains no
92 known functional or structural motifs. Sequence conservation is high in a 315-amino acid stretch
93 within the C-terminal half of the protein, which aligns to shorter proteins in algae and fungi,
94 including the yeast Regulator of Transcription 3 (Rxt3; see dendrogram and sequence alignment in
95 Perrella et al., 2013). Rxt3 co-elutes with the large Rpd3 HDAC-complex in yeast but its function
96 has remained unclear (Carrozza et al., 2005a; Carrozza et al., 2005b). Sequence analysis with JPred
97 (Drozdetskiy et al., 2015) predicts very little secondary structure for HDC1, particularly in the N-
98 terminal part. Intrinsically disordered proteins often act as flexible adaptors for multiple protein
99 interactions (Pazos et al., 2013). It is therefore possible that HDC1 enables multiple protein
100 interactions in HDAC complexes.

101 Here we used a ratiometric Bimolecular Fluorescence Complementation (BiFC) assay in
102 tobacco epidermal cells to test the ability of HDC1 to interact with known and putative members of
103 the HDAC machinery. We then assessed whether a truncated version of HDC1, resembling the
104 shorter, ancestral Rxt3-like proteins, was able to maintain the identified protein interactions and to
105 complement molecular, physiological and developmental phenotypes of *hdc1* knockout plants. The
106 results reveal a potential connection between linker histone H1 and histone deacetylation.

107
108

109 **RESULTS**

110

111 **HDC1 directly interacts with histone-binding protein and associated proteins**

112 Based on the homology search of proteins co-eluting with Rxt3 in yeast complexes and on reported
113 phenotypes and protein interactions in plants (Supplemental Tables 1 and 2), we selected a subset of
114 *A. thaliana* proteins as candidate direct interactors with HDC1: the histone-binding proteins SHL1,
115 ING2 and MSI1 (Mussig et al., 2000; Mussig and Altmann, 2003; Lee et al., 2009; Lopez-Gonzalez
116 et al., 2014; Mehdi et al., 2015), the Sin3-like (SNL) co-repressors SNL2 and SNL3 (Song et al.,
117 2005; Wang et al., 2013), and the Sin3-associated protein SAP18 (Song and Galbraith, 2006). We
118 also included the histone deacetylases (HDA6 , HDA19; (Chen and Wu, 2010)), H3 variants (H3.1.,
119 H3.3; (Jacob et al., 2014)) and H1 variants (H1.1, H1.2 and H1.3; (Ascenzi and Gantt, 1999)) in the
120 interaction assays.

121 The ability of protein pairs to directly interact with each other was investigated using
122 Bimolecular Fluorescence Complementation (BiFC, Figure 1). The proteins were fused to N- or C-
123 terminal halves of Yellow Fluorescent Protein (YFP) and transiently co-expressed in tobacco
124 leaves. We used a ratiometric assay (Grefen and Blatt, 2012) expressing the two fusion proteins and
125 a full-length Red Fluorescent Protein (RFP) from the same vector (2-in-1 vector, Figure 1A). In
126 total, 37 pairwise interactions were assayed in almost a thousand cells. The RFP signal quantifies
127 transgene expression in each cell, and the ratio between YFP and RFP signals allows normalisation
128 and hence direct comparison of interactions between different cells for statistical analysis. In all
129 positive cases the complemented YFP signal was observed inside the nuclei (Figure 1B).

130 To assess whether the Rxt3-like part of the protein is required and sufficient for some or
131 all of the interactions we generated a truncated version of HDC1 spanning amino acids 449 to 764
132 (Rxt3-like; RXT3L, Figure 1C), approximately a third of the full-length protein. Expression of
133 GFP-fusion proteins in tobacco leaves showed that full-length HDC1 and RXT3L were exclusively
134 located in the nuclei. Sequence analysis with PSORT (Nakai and Kanehisa, 1992) highlighted two
135 different putative nuclear retention signals in HDC1 (KR KELKHREWGD RDKDR starting at aa
136 358, and KR RERDGDSEAE RAEKR starting at aa 479). Only the latter was present in RXT3L
137 suggesting that it is sufficient for nuclear localisation. Yeast ScRXT3 contains neither of the motifs
138 and GFP-ScRXT3 was not retained in the nuclei (Supplemental Figure 1), suggesting that the 479
139 motif is necessary for nuclear retention in plant cells.

140 Figure 1 D shows the interaction profile of HDC1 based on YFP/RFP ratios obtained from
141 cells co-expressing HDC1 with candidate interactors. Signals were measured in at least 10 cells
142 from three independently transformed plants. Supplemental Figure 2 shows the respective
143 interaction profiles for SHL1, ING2, MSI1, SAP18, HDA6 and HDA19. The following

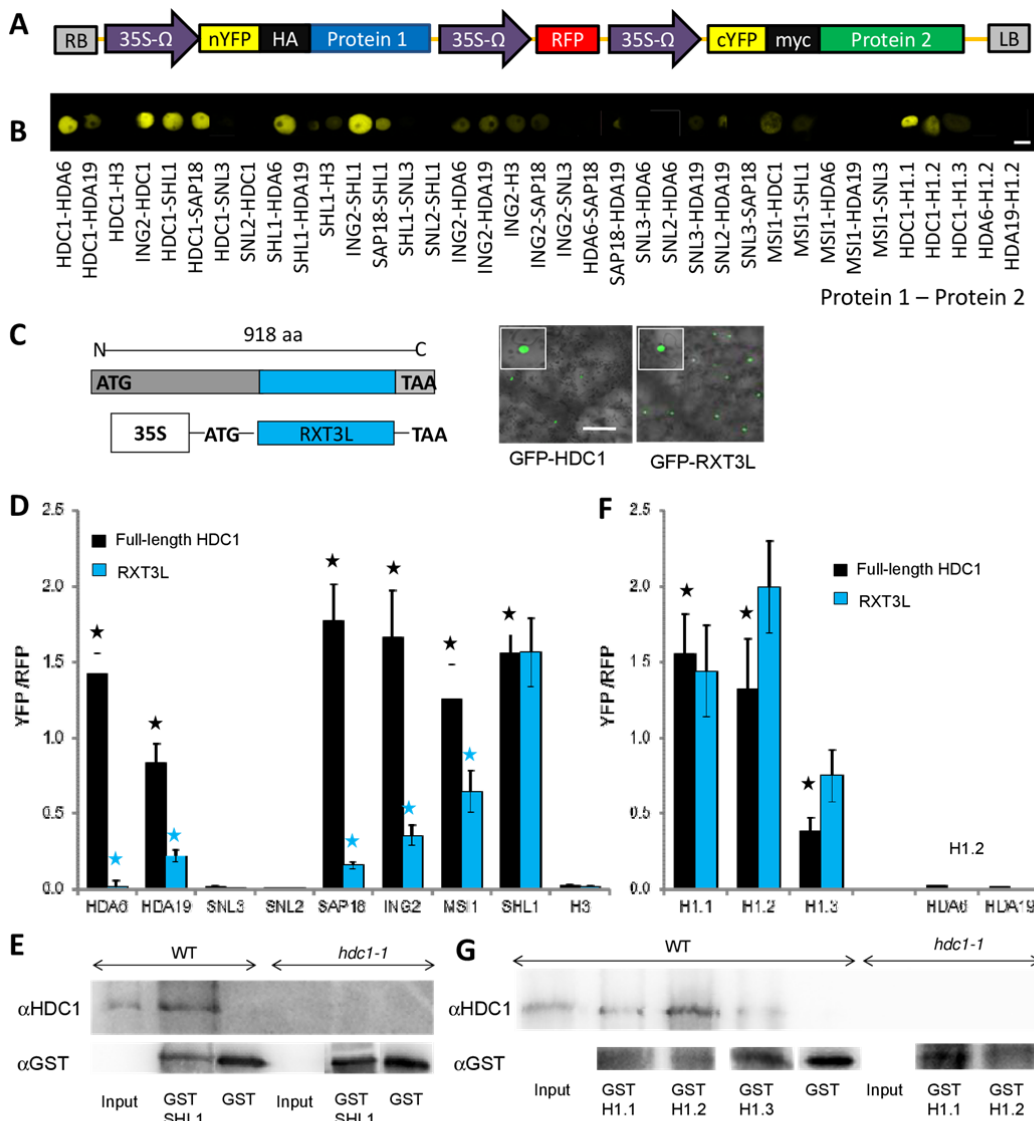


Figure 1: HDC1 directly interacts with several different proteins, and the truncated RXT3L fully maintains the capacity to interact with H3-binding protein SHL1 and with H1 linker histone variants.
A: The 2-in-1 vector for ratiometric BiFC contains N- and C-terminal halves of YFP (nYFP, cYFP) and full-length RFP.
B: Representative YFP signals in nuclei of tobacco epidermis cells transformed with the indicated protein pairs. Bar is 10 μ m.
C: Schematic representation of the truncation construct RXT3L representing a conserved (blue) C-terminal part of full-length HDC1. As for full-length HDC1, GFP-fusion protein of RXT3L shows nuclear localization. Bar is 50 μ m.
D, F: YFP/RFP signal ratio determined in tobacco leaf cells after transient transformation with 2-in-1 BiFC vector containing full length HDC1 (grey bars) or RXT3L (blue bars) together with other proteins. Tested interactors include histone deacetylases HDA6 and 19, Sin3-like co-repressors SNL2 and 3, Sin3-associated protein SAP18, H3-binding proteins SHL1, ING2 and MSI1 (D), as well as H3 and H1 variants H1.1, H1.2 and H1.3 (F). Bars are means \pm SE ($n \geq 30$ cells from three independently transformed plants). Black asterisks (for full-length HDC1) indicate a significant ($p < 0.05$) difference to the signal obtained with SNL3 or H3 (negative controls). Blue asterisks (for RXT3L) indicate significant ($p < 0.05$) difference to the signal obtained with full-length HDC1. The two bars on the right in F are signals obtained for cells transformed with H1.2 and HDA6 or HDA19.
E, G: Western blots showing *in-vivo* pull-down of HDC1 in nuclei-enriched protein samples from wild-type (WT) or HDC1 knockout plants (*hdc1-1*) using GST-SHL1 (E) or GST-H1 variants (G) as bait. The upper panels show the membrane probed with HDC1 antibody (α HDC1). The bottom panels show the membranes re-probed with GST antibody (α GST). As labelled, lanes contain HDC1 only (Input, positive control), pull-down with GST-SHL1 or GST-H1, and pull-down with GST alone (negative control).

Figure 1

144 observations confirmed the validity of the approach. Firstly, for each protein a significant
 145 complementation signal was detected with at least one other protein confirming that all fusion
 146 proteins were properly expressed. Secondly, the complementation signal was always observed

147 inside the nuclei, confirming correct targeting of the fusion proteins. Thirdly, the interaction profiles
148 differed between the proteins tested, confirming specificity of the interactions.

149 As we have previously reported, HDC1 can directly interact with the deacetylases HDA6
150 and HDA19. No direct interaction was found for HDC1 with the co-repressors SNL3 or SNL2 but
151 a strong YFP-complementation signal was recorded when HDC1 was co-expressed with SAP18.
152 SAP18 also failed to directly interact with SNL3 or SNL2 (Supplemental Figure 2). However,
153 SNL2, SNL3 and SAP18 all produced a signal with HDA19 confirming correct expression/folding
154 of the fusion proteins.

155 HDC1 showed interaction with the histone-binding proteins SHL1 and ING2, but not with
156 H3 itself. As expected, SHL1 and ING2 both produced YFP signals with H3 (Supplemental Figure
157 2). They also showed very strong interaction with each other. In addition, SHL1 produced YFP
158 signals when co-expressed with the HDAs or with SAP18. BiFC also showed direct interaction
159 between HDC1 and the H3-binding protein MSI1.

160 HDA19 displayed the broadest interaction profile (Supplemental Figure 2). The strongest
161 signal was obtained with HDC1. Complementation signals with SNL3, SNL2 and SAP18 were
162 weaker than with HDC1 and SHL1, but significantly higher than the signals produced by SNL3
163 with HDC1 or other proteins. Despite previous reports showing pull-down of MSI1 with HDA19
164 we did not record a BiFC signal for these two proteins, suggesting that their interaction is indirect
165 potentially via HDC1. HDA6 had a more selective interaction profile. It strongly interacted with
166 HDC1 and SHL1 but failed to produce BiFC signals with the other proteins tested (Supplemental
167 Figure 2).

168 In summary, the BiFC study identified HDC1 and SHL1 as a potentially important
169 interaction hub in HDAC complexes. To confirm native HDC1-SHL1 assembly we carried out in
170 *in-vivo* pulldown assays with protein extracts from *A. thaliana* leaves using SHL1 as bait. As shown
171 in Figure 1E, SHL1-GST (but not GST alone, 1st negative control) pulled down native HDC1
172 (detected with HDC1-antibody) in protein extracts from wildtype plants, but not from *hdc1-1*
173 knockout plants (2nd negative control). Statistically significant SHL1-HDC1 interaction was
174 confirmed in three independent pulldown experiments (Supplemental Figure 3). HDC1 was not
175 recovered in a pulldown assays using a truncated version of SHL1 (amino acids (aa) 21-137)
176 spanning the histone-binding bromo-adjacent homology (BAH) domain (Supplemental Figure 4).
177 Thus the BAH domain is not involved or not sufficient for the interaction of SHL1 with HDC1.
178 Motivated by our previous finding that HDC1-mediated growth enhancement was maintained under
179 salt stress (Perrella et al, 2013) we also tested interaction between SHL1 and HDC1 in leaf tissue
180 collected from plants subjected to salt (150 mM NaCl for 24 h). Using full-length SHL1 as a bait

181 HDC1 was successfully pulled-down from salt-treated wildtype plants but not from salt-treated
182 *hdc1-1* plants (Supplemental Figure 5).

183

184 **HDC1 interacts with H1**

185 Originally intended as a negative control, we included the linker histone H1 (variant H1.2) in the
186 BiFC assays. To our surprise we found a strong YFP-complementation signal for HDC1 with H1.2
187 (Figure 1F). The interaction was specific because HDC1 did not interact with H3 (see above) and
188 H1.2 did not interact with HDA6 or HDA19 (see right bars in Figure 1F). Upon further testing we
189 found that HDC1 also produced a strong complementation signal with the histone variant H1.1,
190 which is very similar to H1.2, and a weaker signal with the more distinct H1.3 (Figure 1F). *In-vivo*
191 interaction between HDC1 and H1 was confirmed by pull-down assays with protein extracts from
192 Arabidopsis leaves using the H1 variants as bait. As shown in Figure 1G, GST-tagged H1.2 (but not
193 GST alone, 1st negative control) pulled down native HDC1 (detected with HDC1-antibody) in
194 protein extracts from wildtype plants, but not from *hdc1-1* knockout plants (2nd negative control).
195 Fainter HDC1 bands were seen when GST-H.1.1 or GST-H1.3 were used as baits. Pulldowns were
196 repeated four times and statistical analysis of relative band intensities confirmed consistent binding
197 of HDC1 by H1.2 (p = 0.001), more variable binding by H1.1 (p = 0.06), and no binding by H1.3
198 (Supplemental Figure 4). Pull-down of HDC1 with H1.2 was also achieved using leaf material from
199 plants that had been subjected to salt (Supplemental Figure 5). HDC1 was not recovered in
200 pulldown assays with truncated versions of H1.2 representing the N-terminal (aa 1-60), globular
201 (aa 61-129) or C-terminal (aa 130-273) parts of H1.2 (Supplemental Figure 4), indicating that
202 neither of these parts is alone sufficient for interaction.

203

204 **Truncation of HDC1 protein to the yeast RXT3-like core weakens most interactions but does** 205 **not impact on binding of SHL1 or H1**

206 A 315- aa stretch in the C-terminal half of the 918-aa long HDC1 protein aligns to the shorter Rxt3-
207 like proteins in algae and fungi (Perrella et al., 2013). This part of the protein is also more
208 conserved within higher plants than the rest of the protein, and it contains a highly conserved motif
209 of unknown function (PF08642, 602-650 aa in HDC1). To assess whether the Rxt3-like part of the
210 protein is required and sufficient for some or all of the interactions within the plant protein complex
211 we carried out ratiometric BiFC assays and compared the YFP/RFP ratios obtained with RXT3L
212 (blue bars in Fig. 1D and Fig. 1F) with those obtained for full-length HDC1 (black bars). The
213 complementation signals obtained for RXT3L with HDA6, HDA19, ING2, MSI1 or SAP18 were
214 significantly lower than those obtained for full-length HDC1, although still significantly larger than
215 the ones obtained for each protein with SNL3 (Fig. 1D). Thus the truncated protein maintains some

216 affinity for these partners but the interaction is considerably weakened. Strikingly, the truncated
217 RXT3L protein fully retained the ability to directly interact with SHL1, generating a similarly high
218 YFP/RFP signal as full-length HDC1. RXT3L also fully retained the ability to interact with the H1
219 variants (Fig. 1F). The strong signals obtained with SHL1 and H1 also proved that lower signals
220 with the other proteins were not due to weak expression of the RXT3L-YFP fusion protein. The
221 ability of Rxt3L to bind SHL1 and H1 was further confirmed in reciprocal *in-vitro* pull-down
222 experiments, using each of the proteins as bait (Supplemental figure 6).

223

224 **RXT3L partially restores HDC1 functions in plant growth and development**

225 We have previously reported that knockout or overexpression of HDC1 causes a range of
226 phenotypes during plant germination, vegetative growth and flowering (Perrella et al., 2013). To
227 assess the ability of the RXT3L part of the protein to mediate downstream effects of HDC1-
228 dependent histone deacetylation we expressed RXT3L in the HDC1-knockout line *hdc1-1* and in
229 wildtype plants under the control of the 35S promoter. Two homozygous lines from each
230 background were used for the experiments. qPCR analysis with primers in the RXT3L domain
231 (Supplemental Figure 7) confirmed the presence of RXT3L transcript in the overexpressing and
232 complemented lines.

233 Figure 2 shows that the truncated protein was able to carry out functions of full-length
234 HDC1 in germination and growth but was less effective in replacing HDC1 in other functions such
235 as flowering and petiole length. Figure 2A shows that overexpression of RXT3L decreased the
236 ABA- and NaCl-sensitivity of germinating seeds both in wildtype background and in *hdc1-1*
237 background thus mimicking full-length HDC1 (Perrella et al., 2013). RXT3L also reproduced the
238 growth enhancement reported for full-length HDC1; over-expression of RXT3L caused enhanced
239 shoot fresh weight both in wildtype and in *hdc1-1* background (Fig. 2B). We have shown before
240 that enhanced biomass is due to larger leaf size, not to changes in the plastochron (Perrella et al.,
241 2013).

242 RXT3L only partially complemented the delayed flowering phenotype of *hdc1-1*; plant age
243 and number of leaves at bolting were significantly lower than in *hdc1-1* but still significantly higher
244 than in wildtype (Fig. 2C). Another phenotype of *hdc1-1* is compact rosette appearance due to
245 shortened petioles (see inserts in Fig. 2D). Petiole length can be rescued by expression of full-length
246 HDC1 (Perrella et al., 2013) but was not restored by expression of RXT3L in *hdc1-1* (Fig. 2D).
247 Thus, plants expressing RXT3L in *hdc1-1* background were larger than the knockout plants (growth
248 effect) but bulkier than HDC1-complemented or wildtype plants due to short petioles.

249

250

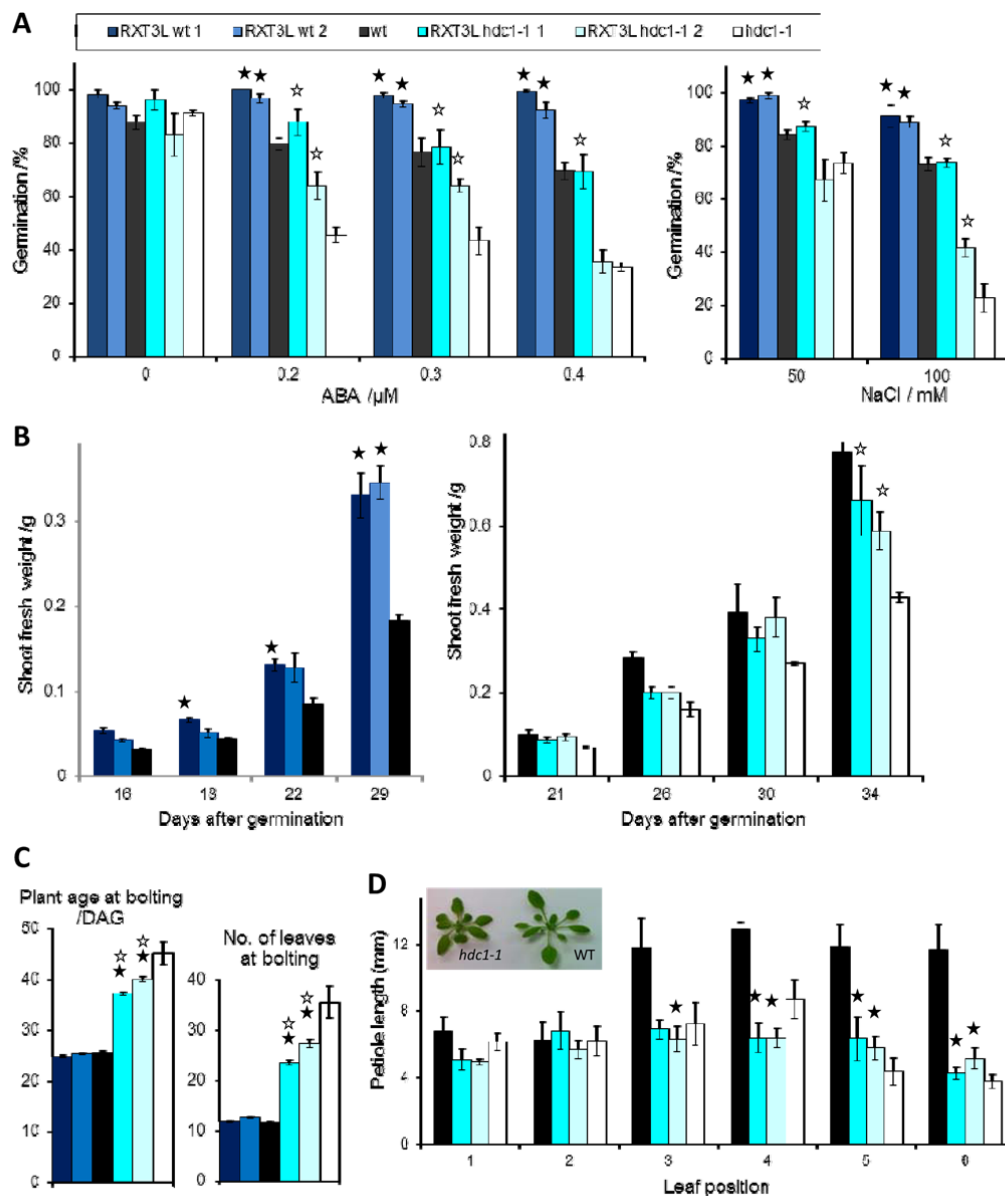


Figure 2: RXT3L complements germination and growth phenotypes of *hdc1* but only partially recovers flowering and is unable to restore petiole extension.

Phenotypes for *Arabidopsis thaliana* wildtype (wt; black), *HDC1*-knockout line (*hdc1-1*, white), two independent lines expressing RXT3L in wt background (RXT3Lwt1,2, dark and light blue) and two independent lines expressing RXT3L in *hdc1-1* background (RXT3Lwt1,2, dark and light turquoise). Significant differences ($p < 0.05$) for Rxt3L-expressing lines against their respective background are indicated with black asterisks for wildtype, and with white asterisks for *hdc1-1*. **A:** Germination rates on agar containing different concentrations of ABA and NaCl. Bars are means \pm SE of at least three plates containing 50 seeds each. *hdc1-1* was significantly different from wildtype in all conditions other than control ($p < 0.05$). **B:** Shoot fresh weight of plants grown in short days at the indicated days after germination. Bars are means \pm SE of three plants harvested each day. *hdc1-1* was significantly different from wildtype from day 26 onwards ($p < 0.05$). **C:** Plant age and number of rosette leaves at bolting (1 cm stem length). Plants were grown in long days. Bars are means \pm SE of 15 plants. *hdc1-1* was significantly different from wildtype for both parameters ($p < 0.05$). **D:** Petiole length of true rosette leaves 1 to 6. Plants were grown in short days. Bars show average petiole length of leaves from three plants \pm SE. *hdc1-1* was significantly different from wildtype for leaves 3-6 ($p < 0.05$). Insert: Picture of *hdc1-1* and wild type plants (3-weeks old).

Figure 2

1

251 DISCUSSION

252 We are only just beginning to appreciate the complexity and regulatory functions of protein
 253 interactions in the nucleus. How DNA and histones recruit the enzymes that modify and regulate
 254 them in a dynamic manner is an active area of research, and understanding how these interactions

255 affect chromatin structure, DNA accessibility and gene transcription remains a challenge. To fully
256 understand the mechanism of histone deacetylation within the context of multi-protein complexes it
257 is essential to investigate those members for which the molecular function is unknown. HDC1 is
258 particularly important because both knockout and overexpression produce measurable effects on
259 histone acetylation levels, gene expression and downstream phenotypes (Perrella et al. 2013). The
260 lack of obvious structural features suggests that HDC1 is intrinsically disordered and could act as a
261 flexible link between multiple proteins.

262 The results of our BiFC study strengthen this hypothesis. We found that HDC1 has the
263 ability to directly interact with several different types of proteins, including histone deacetylases,
264 histone-binding proteins and associated proteins of unknown function. Particular strong interaction
265 was found with the H3-binding protein SHL1, which itself showed a capacity to interact with
266 multiple other proteins. Neither HDC1 nor SHL1 directly interacted with the co-repressor SNL3,
267 which only made close contact with HDA19. The interaction profile suggests that HDC1 associates
268 with the 'histone-binding end' of the complex (Supplemental Figure 8). It is likely that depending
269 on cell-type, developmental stage and environmental conditions, native complexes dynamically
270 assemble into different subsets of the prototype shown in Supplemental Figure 8, and incorporate
271 additional partners not tested here.

272 We also discovered that HDC1 has the capacity to bind H1. H1 is positioned at the edge of
273 nucleosomes, binds to both the nucleosome core and the linker DNA, and correlates with more
274 condensed, less accessible and transcriptionally silent DNA (Ascenzi and Gantt, 1999). In
275 *Arabidopsis thaliana* H1 is encoded by three genes (Ascenzi and Gantt, 1999; Wierzbicki and
276 Jerzmanowski, 2005). H1.1 and H1.2 share 85% identity at the DNA level in the nuclear domain,
277 indicating they might be result of gene duplication. H1.3 is more divergent and it is induced by low
278 light and drought (Ascenzi and Gantt, 1999; Rutowicz et al., 2015). At the phenotypic level, triple
279 knock-out/down of the H1 genes leads to developmental abnormalities with a reduction of plant
280 size, delayed flowering and embryo lethality (Jerzmanowski et al., 2000). Arabidopsis H1s have
281 been found to directly interact with the DNA glycosylase DEMETER which regulates genomic
282 imprinting by demethylating MEDEA promoter in the endosperm (Rea et al., 2012). Furthermore,
283 loss of H1 alters DNA methylation patterns with different effects on euchromatin and
284 heterochromatin (Wierzbicki and Jerzmanowski, 2005; Zemach et al., 2013).). The exact role of H1
285 in DNA modification remains to be elucidated but it has been proposed that it restricts the access of
286 the DNA methyltransferase to the nucleosome (Zemach et al., 2013). The block imposed by H1
287 proteins, mainly within long transposable elements, was overcome by the Swi/Snf chromatin
288 remodeller Decrease of DNA Methylation (DDM) 1, and it was suggested that DDM1 facilitates
289 access of DNA-methylases by removing H1 from the DNA.

290 Based on the above, an interaction between HDC1 and H1 could be functionally interpreted
291 in two ways. In the first hypothesis, HDC1 establishes a physical link between HDAC complexes
292 and H1 thereby enhancing chromatin condensation and repression of the target genes. In the second
293 hypothesis, HDC1 removes H1, similar to DDM, thereby facilitating access of HDAs to the core
294 histone tails. Both functions would benefit from a flexible structure of HDC1. These hypotheses
295 now need to be tested in a genetics approach.

296 Due to the lack of predicted structural motifs or homology to known functional domains in
297 HDC1 it is impossible to pinpoint specific binding sites. In a first gene truncation approach, we
298 found that the capacity to interact with SHL1 and with H1 was fully maintained by the conserved
299 RXT3L part of HDC1 while other interactions were weakened. This could indicate that HDC1 is
300 positioned with the Rxt3-like part at the edge of the nucleosome and the N-terminal part reaching
301 deeper into the complex (Supplemental Figure 8). The phenotypic spectrum of RXT3L indicates
302 that flowering and petiole extension require the full interaction capacity of HDC1, while regulation
303 of germination and growth can be achieved with the partial interaction spectrum maintained by the
304 RXT3L part. It is tempting to consider that the latter phenotypes are evolutionary older and may
305 therefore already been enabled by shorter Rxt3-like proteins in algae, whereas the former, linked to
306 the complex morphology and development of higher plants, required considerable sequence
307 extension of HDC1 to enable a broader protein interaction profile. The results presented here
308 provide a basis for further dissecting the structure-function relationship of HDC1 in different
309 species, and for identifying specific target genes that underpin its diverse physiological and
310 developmental functions.

311
312

313 **MATERIALS AND METHODS**

314 **Plant Materials, Growth Conditions and Treatments**

315 All transgenic lines were generated in *Arabidopsis thaliana* Col-0 background. *hdc1-1* and HDC1-
316 overexpressing lines have been characterised before (Perrella et al. 2013). Homozygous RXT3L-
317 expressing lines were generated from the progeny of wild-type and *hdc1-1* plants transformed with
318 RXT3L part under the control of 35S promoters (see cloning procedures). Plants were grown and
319 treated in controlled growth rooms at a temperature of 22°C and a light intensity of 150 µmol PAR.
320 Plants were grown either in long days (16-h light) or in short days (10-h light) as indicated in text
321 and figure legends. Germination, growth and flowering assays were carried out as described before
322 (Perrella et al. 2013). Petiole and leaf blade length were measured by Image J.

323

324 **Cloning Procedures**

325 Entry clones with full-length HDC1, HDA6, HDA19, SAP18, SHL1, ING2, H3, SNL2 and SNL3,
326 H1.1, H1.2, H1.3, H3.3, MSI1, RXT3L and ScRXT3 with or without stop codon were generated by
327 PCR amplification using primers that contained attB1 and attB2 sites or attB3 and attB4
328 (Supplemental Table 3). For cloning of the RXT3L part, the HDC1 gene sequence from bp 1345 to
329 2292 was amplified. Gel-purified PCR products were introduced into pDONR207/221 (Life
330 Technologies) using BP-clonase II according to the manufacturer's instructions and transferred to
331 destination vectors by recombination using LR-clonase II (Life Technologies). The reaction product
332 was used to transform Top10 bacterial cells. Antibiotic marker resistant colonies were isolated and
333 verified by restriction digest analysis and sequencing. The following plasmids were generated and
334 used in this study: 2x35S::RXT3L in pMDC032 (Curtis and Grossniklaus, 2003), 35S::GFP-HDC1,
335 35S::GFP-RXT3L and 35S::GFP-ScRXT3 in pH7WGF2 (Karimi et al., 2002), 35S::nYFP-protein1
336 /cYFP-protein2 in pBiFCt-2in1-NN (Grefen and Blatt, 2012). For protein expression, the following
337 plasmids were used: pET-Dest42 and pET300/NT-Dest (ThermoFisher), pGEX-4T1 (GE) and a
338 modified pGEX vector containing also a C-terminal histidine tag (Strugnell et al., 1997).

339

340 **Plant Transformation**

341 Plasmids were inserted by heat shock into *Agrobacterium tumefaciens* strain GV3101 pMP90
342 (Koncz and Schell, 1986). *Agrobacterium*-mediated transformation of *Arabidopsis* was performed
343 by the floral dip method (Clough and Bent, 1998). Transient transformation of *Nicotiana*
344 *benthamiana* was achieved by leaf infiltration (Geelen et al., 2002). For ratiometric BiFC assays
345 and co-localization studies, each construct was co-expressed with p19 protein of tomato bushy stunt
346 virus, encoding for a suppressor of gene silencing (Voinnet et al., 2003).

347

348 **Confocal Microscopy**

349 Fluorescence in tobacco epidermal cells was assessed 2 d after infiltration using a CLSM-510-
350 META-UV confocal microscope (Zeiss). For single protein localization, GFP fluorescence was
351 excited at 488 nm with light from an argon laser and collected after passage through an NFT545
352 dichroic mirror with a 505-nm long-pass filter. RFP fluorescence was excited at 543 nm with light
353 from a helium neon laser and was collected after passage through an NFT545 dichroic mirror and a
354 560- to 615-nm band-pass filter. YFP fluorescence was excited at 514 nm with light from an argon
355 laser and collected using lambda mode between 520 and 550 nm. Co-localization plane and line
356 scans were evaluated using Zeiss LSM510AIM software (v3.2).

357

358 **Pull-Down Assays**

359 Protein pulldown were performed as previously described (Perrella et al, 2013). In short, histidine
360 (His)-fused proteins, GST-fused proteins and GST were expressed in Escherichia coli BL21 cells.
361 After induction with 0.5mM mM isopropyl b-D-1-thiogalactopyranoside, cells were harvested and
362 sonicated in lysis buffer. GST-proteins were affinity-purified using Glutathione-Sepharose resin
363 (GE Healthcare) according to the manufacturer's instructions. His-fused proteins were purified
364 using Nickel-NTA resin (Sigma). For pulldowns purified proteins were bound to Glutathione-
365 Sepharose resin and applied to a microcolumn. Nuclei enriched plant lysates were incubated
366 overnight at 4C. For in vitro pulldowns purified proteins bound to Glutathione-Sepharose resin
367 were incubated with His-fused proteins for 4 hours at 4C. After several washes, pulled-down
368 proteins were eluted in Laemmli buffer. For Western blots, the protein samples were boiled, loaded
369 onto SDS-PAGE gel and transferred to nitrocellulose membrane (GE life sciences). Incubation with
370 α HDC, α GST (GE Healthcare) or α His (Cell Signalling Technology) was overnight at dilutions of
371 1:4000, 1:5000 or 1:2000, respectively. Secondary antibody conjugated with horseradish peroxidase
372 was applied for at least 1 hour at room temperature. Finally the membrane was covered with ECL
373 Dura HRP reagent (Thermo Fisher Scientific) and the proteins were detected using a chemi-
374 luminescence imaging platform (Fusion FX, Peqlab). Band intensities were quantified using Image
375 J software.

376

377 **Data analysis**

378 Data were collated and analysed in Excel spreadsheets. Means were calculated across replicates and
379 relevant comparisons were tested using Student t-test. Numbers of replicates and the p-values are
380 indicated in the figure legends.

381

382 **Accession Numbers**

383 Sequence data for genes used in this study can be found in the GenBank/EMBL libraries and in The
384 Arabidopsis Information Resource or in the Saccharomyces Genome database under the following
385 accession numbers: AT5G08450 (HDC1); AT5G63110 (HDA6); AT4G38130 (HDA19);
386 AT2G45640 (SAP18); AT5G15020 (SNL2); AT1G24190 (SNL3); AT4G39100 (SHL1),
387 AT1G54390 (ING2); AT1G09200 (H3.1); AT4G40030 (H3.3); AT1G06760 (H1.1), AT2G30620
388 (H1.2); AT2G18050 (H1.3) AT5G58230 (MSI1); YDL076C (ScRXT3).

389

390 **Supplemental Material**

391 Supplemental File 1 contains Supplemental Figures:

392 **Supplemental Figure 1:** Subcellular localisation of GFP-fusion protein expressed in tobacco.

393 **Supplemental Figure 2:** Interaction profiles of different HDAC complex proteins.

394 **Supplemental Figure 3.** Quantification of HDC1 interaction with H1.2 and SHL1 in *A. thaliana*.
395 **Supplemental Figure 4.** Truncated versions of H1.2 and SHL1 are not binding HDC1.
396 **Supplemental Figure 5.** HDC1 interaction with H1.2 and SHL1 in salt-treated *A. thaliana* plants.
397 **Supplemental Figure 6.** Reciprocal pulldown of Rxt3L/SHL1 and Rxt3L/H1.2.
398 **Supplemental Figure 7:** Transcript levels of the RXT3-like part of HDC.
399 **Supplemental Figure 8:** Visual summary of protein interactions assayed in this study.
400 Supplemental File 2 contains Supplemental Tables:
401 **Supplemental Table 1:** Proteins co-eluting in the *S. cerevisiae* Rpd3L complex
402 **Supplemental Table 2:** Information on selected candidates for interaction with HDC1
403 **Supplemental Table 3:** Primers used for genotyping and cloning
404

405 **ACKNOWLEDGEMENTS**

406 We are grateful to Amparo Ruiz-Prado (University of Glasgow) for horticultural assistance, to
407 George Boswell (University of Glasgow) for maintaining laboratory materials and to Mike Blatt
408 (University of Glasgow) for technical advice.
409

410 **FIGURE LEGENDS**

411 **Figure 1: HDC1 directly interacts with several different proteins, and the truncated RXT3L**
412 **fully maintains the capacity to interact with H3-binding protein SHL1 and with H1 linker**
413 **histone variants.**

414 **A:** The 2-in-1 vector for ratiometric BiFC contains N- and C-terminal halves of YFP (nYFP, cYFP)
415 and full-length RFP. **B:** Representative YFP signals in nuclei of tobacco epidermis cells
416 transformed with the indicated protein pairs. Bar is 10 μm . **C:** Schematic representation of the
417 truncation construct RXT3L representing a conserved (blue) C-terminal part of full-length HDC1.
418 As for full-length HDC1, GFP-fusion protein of RXT3L shows nuclear localization. Bar is 50 μm .
419 **D, F:** YFP/RFP signal ratio determined in tobacco leaf cells after transient transformation with 2-in-
420 1 BIFC vector containing full length HDC1 (grey bars) or RXT3L (blue bars) together with other
421 proteins. Tested interactors include histone deacetylases HDA6 and 19, Sin3-like co-repressors
422 SNL2 and 3, Sin3-associated protein SAP18, H3-binding proteins SHL1, ING2 and MSI1 (D), as
423 well as H3 and H1 variants H1.1, H1.2 and H1.3 (F). Bars are means \pm SE ($n \geq 30$ cells from three
424 independently transformed plants). Black asterisks (for full-length HDC1) indicate a significant ($p <$
425 0.05) difference to the signal obtained with SNL3 or H3 (negative controls). Blue asterisks (for
426 RXT3L) indicate significant ($p < 0.05$) difference to the signal obtained with full-length HDC1. The
427 two bars on the right in F are signals obtained for cells transformed with H1.2 and HDA6 or
428 HDA19. **E, G:** Western blots showing *in-vivo* pulldown of HDC1 in nuclei-enriched protein

429 samples from wild-type (WT) or HDC1 knockout plants (*hdc1-1*) using GST-SHL1 (B) or GST-H1
430 variants (D) as bait. The upper panels show the membrane probed with HDC1 antibody (α HDC1).
431 The bottom panels show the membranes re-probed with GST antibody (α GST). As labelled, lanes
432 contain HDC1 only (Input, positive control), pull-down with GST-SHL1 or GST-H1, and pull-
433 down with GST alone (negative control).

434

435 **Figure 2: RXT3L complements germination and growth phenotypes of *hdc1* but only partially**
436 **recovers flowering and is unable to restore petiole extension.**

437 Phenotypes for *Arabidopsis thaliana* wildtype (wt; black), HDC1-knockout line (*hdc1-1*, white),
438 two independent lines expressing RXT3L in wt background (RXT3Lwt1,2, dark and light blue) and
439 two independent lines expressing RXT3L in *hdc1-1* background (RXT3Lwt1,2dark and light
440 turquoise) Significant differences ($p < 0.05$) for Rxt3L-expressing lines against their respective
441 background are indicated with black asterisks for wildtype, and with white asterisks for *hdc1-1*. **A:**
442 Germination rates on agar containing different concentrations of ABA and NaCl. Bars are means \pm
443 SE of at least three plates containing 50 seeds each. *hdc1-1* was significantly different from
444 wildtype in all conditions other than control ($p < 0.05$). **B:** Shoot fresh weight of plants grown in
445 short days at the indicated days after germination. Bars are means \pm SE of three plants harvested
446 each day. *hdc1-1* was significantly different from wildtype from day 26 onwards ($p < 0.05$). **C:**
447 Plant age and number of rosette leaves at bolting (1 cm stem length). Plants were grown in long
448 days. Bars are means \pm SE of 15 plants. *hdc1-1* was significantly different from wildtype for both
449 parameters ($p < 0.05$). **D:** Petiole length of true rosette leaves 1 to 6. Plants were grown in short
450 days. Bars show average petiole length of leaves from three plants \pm SE. *hdc1-1* was significantly
451 different from wildtype for leaves 3-6 ($p < 0.05$). Insert: Picture of *hdc1-1* and wild type plants (3-
452 weeks old).

453

454

Parsed Citations

Ascenzi R, Gantt JS (1999) Molecular genetic analysis of the drought-inducible linker histone variant in Arabidopsis thaliana. Plant Molecular Biology 41: 159-169

Pubmed: [Author and Title](#)
CrossRef: [Author and Title](#)
Google Scholar: [Author Only](#) [Title Only](#) [Author and Title](#)

Ascenzi R, Gantt JS (1999) Subnuclear distribution of the entire complement of linker histone variants in Arabidopsis thaliana. Chromosoma 108: 345-355

Pubmed: [Author and Title](#)
CrossRef: [Author and Title](#)
Google Scholar: [Author Only](#) [Title Only](#) [Author and Title](#)

Chen LT, Luo M, Wang YY, Wu KQ (2010) Involvement of Arabidopsis histone deacetylase HDA6 in ABA and salt stress response. Journal of Experimental Botany 61: 3345-3353

Pubmed: [Author and Title](#)
CrossRef: [Author and Title](#)
Google Scholar: [Author Only](#) [Title Only](#) [Author and Title](#)

Chen LT, Wu KQ (2010) Role of histone deacetylases HDA6 and HDA19 in ABA and abiotic stress response. Plant Signaling & Behavior 5: 1318-1320

Pubmed: [Author and Title](#)
CrossRef: [Author and Title](#)
Google Scholar: [Author Only](#) [Title Only](#) [Author and Title](#)

Clough SJ, Bent AF (1998) Floral dip: a simplified method for Agrobacterium-mediated transformation of Arabidopsis thaliana. Plant Journal 16: 735-743

Pubmed: [Author and Title](#)
CrossRef: [Author and Title](#)
Google Scholar: [Author Only](#) [Title Only](#) [Author and Title](#)

Curtis MD, Grossniklaus U (2003) A gateway cloning vector set for high-throughput functional analysis of genes in planta. Plant Physiology 133: 462-469

Pubmed: [Author and Title](#)
CrossRef: [Author and Title](#)
Google Scholar: [Author Only](#) [Title Only](#) [Author and Title](#)

Derkacheva M, Steinbach Y, Wildhaber T, Mozgova I, Mahrez W, Nanni P, Bischof S, Grisse W, Hennig L (2013) Arabidopsis MSI1 connects LHP1 to PRC2 complexes. Embo Journal 32: 2073-2085

Pubmed: [Author and Title](#)
CrossRef: [Author and Title](#)
Google Scholar: [Author Only](#) [Title Only](#) [Author and Title](#)

Drozdetskiy A, Cole C, Procter J, Barton GJ (2015) JPred4: a protein secondary structure prediction server. Nucleic Acids Research 43: W389-W394

Pubmed: [Author and Title](#)
CrossRef: [Author and Title](#)
Google Scholar: [Author Only](#) [Title Only](#) [Author and Title](#)

Geelen D, Leyman B, Batoko H, Di Sansabastiano GP, Moore I, Blatt MR (2002) The abscisic acid-related SNARE homolog NtSyr1 contributes to secretion and growth: Evidence from competition with its cytosolic domain. Plant Cell 14: 387-406

Pubmed: [Author and Title](#)
CrossRef: [Author and Title](#)
Google Scholar: [Author Only](#) [Title Only](#) [Author and Title](#)

Grefen C, Blatt MR (2012) A2in1 cloning system enables ratiometric Bimolecular Fluorescence Complementation (rBiFC). Biotechniques 53: 311-314

Pubmed: [Author and Title](#)
CrossRef: [Author and Title](#)
Google Scholar: [Author Only](#) [Title Only](#) [Author and Title](#)

Hergeth SP, Schneider R (2015) The H1 linker histones: multifunctional proteins beyond the nucleosomal core particle. Embo Reports 16: 1439-1453

Pubmed: [Author and Title](#)
CrossRef: [Author and Title](#)
Google Scholar: [Author Only](#) [Title Only](#) [Author and Title](#)

Jacob Y, Bergamin E, Donoghue MTA, Mongeon V, LeBlanc C, Voigt P, Underwood CJ, Brunzelle JS, Michaels SD, Reinberg D, Couture JF, Martienssen RA (2014) Selective Methylation of Histone H3 Variant H3.1 Regulates Heterochromatin Replication. Science 343: 1249-1253

Pubmed: [Author and Title](#)
CrossRef: [Author and Title](#)
Google Scholar: [Author Only](#) [Title Only](#) [Author and Title](#)

Jerzmanowski A, Przewlaka M, Grasser KD (2000) Linker histones and HMG1 proteins of higher plants. Plant Biology 2: 586-597

Pubmed: [Author and Title](#)
CrossRef: [Author and Title](#)
Google Scholar: [Author Only](#) [Title Only](#) [Author and Title](#)

- Karimi M, Inze D, Depicker A (2002) GATEWAY(TM) vectors for Agrobacterium-mediated plant transformation. Trends in Plant Science 7: 193-195**
Pubmed: [Author and Title](#)
CrossRef: [Author and Title](#)
Google Scholar: [Author Only](#) [Title Only](#) [Author and Title](#)
- Koncz C, Schell J (1986) THE PROMOTER OF TL-DNA GENE 5 CONTROLS THE TISSUE-SPECIFIC EXPRESSION OF CHIMERIC GENES CARRIED BY A NOVEL TYPE OF AGROBACTERIUM BINARY VECTOR. Molecular & General Genetics 204: 383-396**
Pubmed: [Author and Title](#)
CrossRef: [Author and Title](#)
Google Scholar: [Author Only](#) [Title Only](#) [Author and Title](#)
- Kouzarides T (2007) Chromatin modifications and their function. Cell 128: 693-705**
Pubmed: [Author and Title](#)
CrossRef: [Author and Title](#)
Google Scholar: [Author Only](#) [Title Only](#) [Author and Title](#)
- Lee WY, Lee D, Chung WJ, Kwon CS (2009) Arabidopsis ING and Atfin1-like protein families localize to the nucleus and bind to H3K4me3/2 via plant homeodomain fingers. Plant Journal 58: 511-524**
Pubmed: [Author and Title](#)
CrossRef: [Author and Title](#)
Google Scholar: [Author Only](#) [Title Only](#) [Author and Title](#)
- Liu CY, Lu FL, Cui X, Cao XF (2010) Histone Methylation in Higher Plants. In S Merchant, WR Briggs, D Ort, eds, Annual Review of Plant Biology, Vol 61, Vol 61. Annual Reviews, Palo Alto, pp 395-420**
Pubmed: [Author and Title](#)
CrossRef: [Author and Title](#)
Google Scholar: [Author Only](#) [Title Only](#) [Author and Title](#)
- Lopez-Gonzalez L, Mouriz A, Narro-Diego L, Bustos R, Martinez-Zapater JM, Jarillo JA, Pineiro M (2014) Chromatin-Dependent Repression of the Arabidopsis Floral Integrator Genes Involves Plant Specific PHD-Containing Proteins. Plant Cell 26: 3922-3938**
Pubmed: [Author and Title](#)
CrossRef: [Author and Title](#)
Google Scholar: [Author Only](#) [Title Only](#) [Author and Title](#)
- Mehdi S, Derkacheva M, Ramström M, Kralemann L, Bergquist J, Hennig L (2015) The WD40 domain protein MSI1 functions in a histone deacetylase complex to fine-tune abscisic acid signaling. Plant Cell 28: 42-54**
Pubmed: [Author and Title](#)
CrossRef: [Author and Title](#)
Google Scholar: [Author Only](#) [Title Only](#) [Author and Title](#)
- Mussig C, Altmann T (2003) Changes in gene expression in response to altered SHL transcript levels. Plant Molecular Biology 53: 805-820**
Pubmed: [Author and Title](#)
CrossRef: [Author and Title](#)
Google Scholar: [Author Only](#) [Title Only](#) [Author and Title](#)
- Mussig C, Kauschmann A, Clouse SD, Altmann T (2000) The Arabidopsis PHD-finger protein SHL is required for proper development and fertility. Molecular and General Genetics 264: 363-370**
Pubmed: [Author and Title](#)
CrossRef: [Author and Title](#)
Google Scholar: [Author Only](#) [Title Only](#) [Author and Title](#)
- Nakai K, Kanehisa M (1992) A knowledge base for predicting protein localization sites in eukaryotic cells. Genomics 14: 897-911.**
Pubmed: [Author and Title](#)
CrossRef: [Author and Title](#)
Google Scholar: [Author Only](#) [Title Only](#) [Author and Title](#)
- Over RS, Michaels SD (2014) Open and Closed: The Roles of Linker Histones in Plants and Animals. Molecular Plant 7: 481-491**
Pubmed: [Author and Title](#)
CrossRef: [Author and Title](#)
Google Scholar: [Author Only](#) [Title Only](#) [Author and Title](#)
- Pazos F, Pietrosevoli N, Garcia-Martin JA, Solano R (2013) Protein intrinsic disorder in plants. Frontiers in Plant Science 4**
Pubmed: [Author and Title](#)
CrossRef: [Author and Title](#)
Google Scholar: [Author Only](#) [Title Only](#) [Author and Title](#)
- Perrella G, Lopez Vernaza MA, Carr C, Sani E, Gossele V, Verduyn C, Kellermeier F, Hannah M-K, Amtmann A (2013) Histone deacetylase complex1 expression level titrates plant growth and abscisic acid sensitivity in Arabidopsis. Plant Cell 25: 3491-3505**
Pubmed: [Author and Title](#)
CrossRef: [Author and Title](#)
Google Scholar: [Author Only](#) [Title Only](#) [Author and Title](#)
- Pfluger J, Wagner D (2007) Histone modifications and dynamic regulation of genome accessibility in plants. Current Opinion in Plant Biology 10: 645-652**
Pubmed: [Author and Title](#)
CrossRef: [Author and Title](#)
Google Scholar: [Author Only](#) [Title Only](#) [Author and Title](#)
- Rea M, Zheng WG, Chen M, Braud C, Bhangu D, Rognan TN, Xiao WY (2012) Histone H1 affects gene imprinting and DNA**

methylation in Arabidopsis. Plant Journal 71: 776-786

Pubmed: [Author and Title](#)

CrossRef: [Author and Title](#)

Google Scholar: [Author Only Title Only Author and Title](#)

Roudier F, Teixeira FK, Colot V (2009) Chromatin indexing in Arabidopsis: an epigenomic tale of tails and more. Trends in Genetics 25: 511-517

Pubmed: [Author and Title](#)

CrossRef: [Author and Title](#)

Google Scholar: [Author Only Title Only Author and Title](#)

Rutowicz K, Puzio M, Halibart-Puzio J, Lirski M, Kotlinski M, Kroten MA, Knizewski L, Lange B, Muszewska A, Sniegowska-Swierk K, Koscielniak J, Iwanicka-Nowicka R, Buza K, Janowiak F, Zmuda K, Joesaar I, Laskowska-Kaszub K, Fogtman A, Kollist H, Zielenkiewicz P, Tiurnyn J, Siedlecki P, Swiezewski S, Ginalski K, Koblowska M, Archacki R, Wilczynski B, Rapacz M, Jerzmanowski A (2015) A Specialized Histone H1 Variant Is Required for Adaptive Responses to Complex Abiotic Stress and Related DNA Methylation in Arabidopsis. Plant Physiol 169: 2080-2101

Pubmed: [Author and Title](#)

CrossRef: [Author and Title](#)

Google Scholar: [Author Only Title Only Author and Title](#)

Song CP, Agarwal M, Ohta M, Guo Y, Halfter U, Wang PC, Zhu JK (2005) Role of an Arabidopsis AP2/EREBP-type transcriptional repressor in abscisic acid and drought stress responses. Plant Cell 17: 2384-2396

Pubmed: [Author and Title](#)

CrossRef: [Author and Title](#)

Google Scholar: [Author Only Title Only Author and Title](#)

Song CP, Galbraith DW (2006) AtSAP18, an orthologue of human SAP18, is involved in the regulation of salt stress and mediates transcriptional repression in Arabidopsis. Plant Molecular Biology 60: 241-257

Pubmed: [Author and Title](#)

CrossRef: [Author and Title](#)

Google Scholar: [Author Only Title Only Author and Title](#)

Strugnell SA, Wefling BA, DeLuca HF (1997) A modified pGEX vector with a C-terminal histidine tag: Recombinant double-tagged protein obtained in greater yield and purity. Analytical Biochemistry 254: 147-149

Pubmed: [Author and Title](#)

CrossRef: [Author and Title](#)

Google Scholar: [Author Only Title Only Author and Title](#)

Tanaka M, Kikuchi A, Kamada H (2008) The Arabidopsis histone deacetylases HDA6 and HDA19 contribute to the repression of embryonic properties after germination. Plant Physiology 146: 149-161

Pubmed: [Author and Title](#)

CrossRef: [Author and Title](#)

Google Scholar: [Author Only Title Only Author and Title](#)

Voinnet O, Rivas S, Mestre P, Baulcombe D (2003) An enhanced transient expression system in plants based on suppression of gene silencing by the p19 protein of tomato bushy stunt virus. Plant Journal 33: 949-956

Pubmed: [Author and Title](#)

CrossRef: [Author and Title](#)

Google Scholar: [Author Only Title Only Author and Title](#)

Wang Z, Cao H, Sun YZ, Li XY, Chen FY, Carles A, Li Y, Ding M, Zhang C, Deng X, Soppe WJJ, Liu YX (2013) Arabidopsis Paired Amphipathic Helix Proteins SNL1 and SNL2 Redundantly Regulate Primary Seed Dormancy via Abscisic Acid-Ethylene Antagonism Mediated by Histone Deacetylation. Plant Cell 25: 149-166

Pubmed: [Author and Title](#)

CrossRef: [Author and Title](#)

Google Scholar: [Author Only Title Only Author and Title](#)

Wierzbicki AT, Jerzmanowski A (2005) Suppression of histone H1 genes in Arabidopsis results in heritable developmental defects and Stochastic changes in DNA methylation. Genetics 169: 997-1008

Pubmed: [Author and Title](#)

CrossRef: [Author and Title](#)

Google Scholar: [Author Only Title Only Author and Title](#)

Yu CW, Liu XC, Luo M, Chen CY, Lin XD, Tian G, Lu Q, Cui YH, Wu KQ (2011) HISTONE DEACETYLASE 6 Interacts with FLOWERING LOCUS D and Regulates Flowering in Arabidopsis. Plant Physiology 156: 173-184

Pubmed: [Author and Title](#)

CrossRef: [Author and Title](#)

Google Scholar: [Author Only Title Only Author and Title](#)

Zemach A, Kim MY, Hsieh PH, Coleman-Derr D, Eshed-Williams L, Thao K, Harmer SL, Zilberman D (2013) The Arabidopsis Nucleosome Remodeler DDM1 Allows DNA Methyltransferases to Access H1-Containing Heterochromatin. Cell 153: 193-205

Pubmed: [Author and Title](#)

CrossRef: [Author and Title](#)

Google Scholar: [Author Only Title Only Author and Title](#)